JOURNAL OF MATERIALS SCIENCE **36** (2001) 3715–3720

Calculation of elastic properties of natural fibers

JOCHEN GASSAN*,**
University of Kassel, Institut für Werkstofftechnik, Kassel, Germany
E-mail: jochen.gassan@sommer-allibert.com

ANDRIS CHATE
Institute of Computer Analysis of Structure, Riga Technical University, Kalku iela 1, LV-1658 Riga, Latvia

ANDRZEJ K. BLEDZKI
University of Kassel, Institut für Werkstofftechnik, Kassel, Germany

This article deals with the calculation of the elastic properties of cellulose based natural fibers by using two different types of idealization and assumptions. One model (model A) bases on antisymmertrical laminated structure, while the second one (model B) bases on a thick laminated composite tube model. Model B is able to take into account the elliptic geometry, the hollow based structure of the cross section of the fiber cell. The calculated relationships between spiral angle and modulus in fiber axis by model A fits successful experimental data for holocellulose fibers which were published elsewhere. In general, modulus in fiber axis decreases with increasing spiral angle as well as the degree of anisotropy, while shear modulus reaches a maximum for a spiral angle of 45°. Fiber cell modulus increases linear with increasing cellulose content for both, the calculated (model A) and measured values. The correlation between experimental data and calculation ones was not as high as in the case of modulus versus spiral angle. The discrepancy between model A and a more real cross section is calculated (model B) with roughly 30%.

1. Introduction

In the search for an understanding of the elasticity of natural and wood fibers, it is essential to derive theoretical tools to link the structure and mechanical properties of the components into a comprehensive composite model.

In recent years, such structure-property models had been described in terms of various models of structural arrangements of their components [1–9].

One of the first theories had been presented by Hearle [1], where a mechanics of extension of fibers was considered in terms of a spiral arrangement of crystalline fibrils embedded in the non-crystalline matrix on a two-phase level, by taking into account layer S_2. Hearle considered, that on extension of the fiber, the deformation might occur by an increase in length of fibrils and of the non-crystalline regions in between and by extension like a spiral spring, with bending and twisting of the fibrils. This model was developed and used by Hearle in some of his next papers [2–4].

A cell-wall laminated model of a natural (wood) fiber had been presented by Salmén and de Ruvo [6] and Salmén *et al*. [7]. They modelled the structure of a single wood fiber cell as multilayer material with layers of cellulose microfibrils at different angles with respect to the fiber axis. It is suggested that the wood fiber is a composite of the three polymers cellulose, hemicellulose and lignin, in which the unidirectional cellulose microfibrils constitute the reinforcing elements in the matrix blend of hemicellulose and lignin. The structure of such a fiber was built as multi-ply construction with layers P, S_1, S_2 and S_3 of cellulose microfibrils at different angles to the fiber axis. In this model, well-beaten fiber was able be considered to be collapsed, i.e., the square fiber has been flattened so that its inner surfaces contact each other. In this case, the angle of the fibrils in a layer in the front fiber wall is opposite to that in the back fiber wall. Thus the fiber was able to be viewed as an anti-symmetric laminate by using classical laminated theory for estimating the elastic properties of such fiber structure.

Koponen *et al*. [8, 9] calculated the elastic constants of the cell wall with equitations derived from a 3-dimensional case, where the layered media was replaced by an equivalent homogeneous material. In this model the cell wall, in similar as in [6, 7], consists from the layers P, S_1, S_2 and S_3, where two adjacent cell walls were examined as a unit.

A overview about the developments in cell wall models are given by Salmén *et al*. [6]. Some typical spiral

* Author to whom all correspondence should be addressed.
** *Present address*: SAI Automotive SAL GmbH.

TABLE I Cellulose content and spiral angle of different natural fibers [10–12]

Fiber	Spiral angle [°]	Cellulose content [wt.-%]
Banana	11	65
Coir	30–49	43
Flax	6–10	64–71
Hemp	6	—
Jute	8	61–72
Pineapple	8–14	81
Sisal	10–25	66–70
Ramie	8	69–83

angles and cellulose contents of different natural fibers are given in Table I.

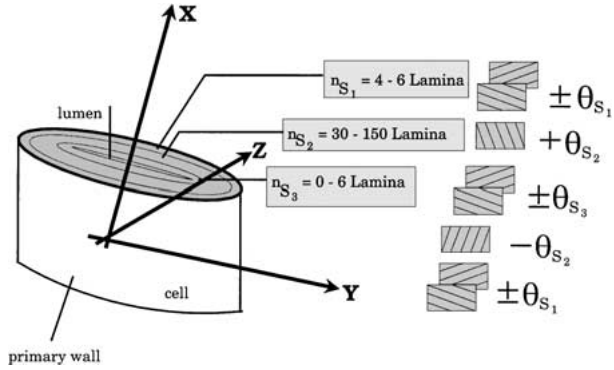

Figure 2 Illustration of one single fiber cell as general model for modelling based on [2, 6, 7, 12,14].

2. Developed models and modelling

2.1. Basic idea

With regard to the fact that natural fibers (e.g., wood fibers [13]) possess a finite hole in the centre of the cell, the fiber structure has a finite width and rather substantial thickness (Fig. 1 for a jute fiber for instance). It means that a laminated fiber model (using classical laminated theory) is far from the realistic structure of a natural fiber.

Because of this, two structural based models for a natural fiber cell are presented throughout this study. For both models the structure according to Fig. 2 was used. The layers S_1 up to S_3 consist of cellulose microfibrils embedded in the matrix of hemicellulose and lignin by taking into account the different spiral angles and layer thickness of each of the layers.

In the case of the laminated plate model, a 8-layer antisymmetrical laminated structure (P, S_1, S_2, S_3, S_3, S_2, S_1, P) is considered. Because the state of stress in the laminate under loading is three dimensional, it is necessary to formulate three dimensional stress-strain relationships. Taking into account the lumen (as hole), a more realistic model seems to be the thick laminated composite tube model. In the laminated tube model, the natural fiber is considered as thick laminated composite tube, which consists of four layers (P, S_1, S_2, and S_3). In this case, finite element method is used for the calculation. Here, each layer of the fiber cell has been modelled as a three-dimensional finite element. In our case, the FEM-program has been developed estimating the longitudinal elastic modulus and longitudinal stiffness, respectively, for a natural fiber cell with an elliptic cross section. The FEM-program further allows to calculate the elastic properties for a geometrical range of the cross section

$$0.1 \leq b/a \leq 1,$$

where a is the largest half axes of the ellipse and b is the smallest half axes of the ellipse. If $b/a = 1$, than

Figure 1 SEM study on jute fiber.

TABLE II Elastic properties of cellulose, hemicellulose, and lignin [6, 7, 14]

	E_{11} [kN/mm^2]	E_{22} [kN/mm^2]	G_{12} [kN/mm^2]	ν_{12} [/]
Cellulose I	134 74–168	27.2	4.4	0.1
Hemicellulose	8	4	2	0.2
Lignin	4	4	1.5	0.33

the cross section of fiber cell is circular. If $b/a = 0.1$, than the results of the FEM modelling strive to the results of the results from the 8-layered antisymmetrical laminated model.

2.2. Modelling

As mentioned before, two models were developed and discussed in this paper for estimating the elastic properties of a natural fiber from the properties of its polymeric constituents: lignin, cellulose and hemicellulose (Table II).

A. Laminated plate model

In this model, a natural fiber cell (Fig. 2) is considered as antisymmetrical laminated structure

$$\left(\beta_{\text{lignin}}/\beta_{S_1}/\beta_{S_2}/\beta_{S_3}/-\beta_{S_3}/-\beta_{S_2}/-\beta_{S_1}/-\beta_{\text{lignin}}\right)$$

with the constitutive relations as [15, 16]:

$$\begin{Bmatrix} N_{xx} \\ N_{yy} \\ N_{xy} \\ M_{xx} \\ M_{yy} \\ M_{xy} \\ Q_y \\ Q_x \end{Bmatrix} = \begin{bmatrix} Q_{11} & Q_{12} & Q_{16} & B_{11} & B_{12} & B_{16} & 0 & 0 \\ & Q_{22} & Q_{26} & B_{12} & B_{22} & B_{26} & 0 & 0 \\ & & Q_{66} & B_{16} & B_{26} & B_{66} & 0 & 0 \\ & & & D_{11} & D_{12} & D_{16} & 0 & 0 \\ & & & & D_{22} & D_{26} & 0 & 0 \\ & symm. & & & & D_{66} & 0 & 0 \\ & & & & & & Q_{44} & Q_{45} \\ & & & & & & & Q_{55} \end{bmatrix} \times \begin{Bmatrix} \Omega_{xx} \\ \Omega_{yy} \\ 2\Omega_{xy} \\ \chi_{xx} \\ \chi_{yy} \\ 2\chi_{xy} \\ 2\Omega_{y3} \\ 2\Omega_{x3} \end{Bmatrix} \tag{A1}$$

or

$$\{N\} = [D]\{E\}$$

where

$$Q_{ij} = \sum_{L=1}^{K} A_{ij}^{(L)}(z_L - z_{L-1});$$

$$B_{ij} = \frac{1}{2}\sum_{L=1}^{K} A_{ij}^{(L)}\left(z_L^2 - z_{L-1}^2\right);$$

$$D_{ij} = \frac{1}{3}\sum_{L=1}^{K} A_{ij}^{(L)}\left(z_L^3 - z_{L-1}^3\right)$$

and components of axial forces (N_{xx}, N_{yy}, N_{xy}), moments (M_{xx}, M_{yy}, M_{xy}) and shear forces (Q_y, Q_x) of the laminated structure are defined in a standard way.

Here, $A_{ij}^{(L)}$ is defined as the stiffness of the L-th lamina, z_L as the co-ordinate of the laminas, Ω_{xx}, Ω_{yy}, $2\Omega_{xy}$ are membrane strains, χ_{xx}, χ_{yy}, $2\chi_{xy}$ are bending curvatures, and $2\Omega_{y3}$, $2\Omega_{x3}$ are shear strains [15, 16].

The effective elastic constants of a natural fiber (as laminated structure) can be determined by the inverse matrix of $[D]$ from Equation A1

$$[d] = [D]^{-1} \tag{A2}$$

This inverse matrix takes into account the stress coupling that may occur from various orientations of fibrils and variation of fiber structure. The effective moduli of 'laminated' fiber structure are

$$E_x = \frac{1}{hq_{11}}, \quad E_y = \frac{1}{hq_{22}}, \quad G_{xy} = \frac{1}{hq_{66}}, \quad \nu_{xy} = -\frac{E_x q_{12}}{h} \tag{A3}$$

here, h is the total thickness of the structure and $q_{11}, q_{22}, q_{12}, q_{66}$ are taken from matrix $[d]$

$$[d] = \begin{bmatrix} q_{11} & q_{12} & q_{16} & b_{11} & b_{12} & b_{16} & 0 & 0 \\ & q_{22} & q_{26} & b_{12} & b_{22} & b_{26} & 0 & 0 \\ & & q_{66} & b_{16} & b_{26} & b_{66} & 0 & 0 \\ & & & d_{11} & d_{12} & d_{16} & 0 & 0 \\ & & & & d_{22} & d_{26} & 0 & 0 \\ & symm. & & & & d_{66} & 0 & 0 \\ & & & & & & q_{44} & q_{45} \\ & & & & & & & q_{55} \end{bmatrix}$$

B. Thick laminated tube model

Taking into account the fact that the structure of a fiber cell has a 'hole' (lumen) and substantial thickness, using a thick laminated composite tube model seems to be more realistic. For this, the natural fiber cell is considered as thick laminated tube with four layers

$$\left(\beta_{\text{lignin}}/\beta_{S_1}/\beta_{S_2}/\beta_{S_3}\right)$$

It is further considered that the cell, which consists of an anisotropic homogeneous medium, exhibits the same strain energy U^{eq} in deformation state as actual natural fiber U (as laminated material), thus

$$U = U^{eq} \tag{B1}$$

Let us denote the macro strains of a fiber as homogeneous medium by E_{ij} and corresponding macro stresses by Φ_{ij}, then the deformation energy of a natural fiber can be treated as equivalent material (macro homogeneous body) as follows

$$U^{eq} = \frac{1}{2}\int_V \Phi_{ij}E_{ij}\,dV = \frac{1}{2}\int_V S_{ijkl}\Phi_{ij}\Phi_{kl}\,dV \tag{B2}$$

where S_{ijkl} are compliance tensors [17].

On the other hand, the deformation energy of a natural fiber (thick laminated composite tube as nonhomogeneous medium) is computed using FEM. In this case, the corresponding deformation energy can be derived from

$$U = \frac{1}{2}\int_V \sigma_{ij}\varepsilon_{ij}\,dV \tag{B3}$$

where σ_{ij} and ε_{ij} are the micro stresses and micro strains in a fiber, respectively.

For example, to determine the elastic constant E_x, the following boundary conditions must be considered

$$\Phi_{xx} = 1; \quad \Phi_{yy} = \Phi_{zz} = \Phi_{xy} = \Phi_{xz} = \Phi_{yz} = 0 \tag{B4}$$

Taking into account (B2, B3) and boundary conditions (B4), Equation B1 can be rewritten as

$$\frac{1}{2}S_{xx}(\Phi_{xx})^2V = \frac{1}{2}\frac{(\Phi_{xx})^2}{E_x}V = U \tag{B5}$$

where U is the deformation energy of a natural fiber (calculated by FEM) for the boundary conditions (B4). Because the stress state in these layers under loading will be a 3-D one, three-dimensional curved isoparametric solid finite elements with 20 nodal points [18] were used for modelling the natural fiber. From (B5) follows

$$E_x = \frac{(\Phi_{xx})^2V}{2U} \tag{B6}$$

3. Results and discussion

3.1. Spiral angle dependency

Since the S_2 layer of the cell wall represents such a large proportion of the fiber wall, the spiral angle of this layer will have a pronounced influence on the properties of the fiber. This fact was clearly demonstrated in earlier papers [1–4, 6].

For pure cellulose a modulus from 74–168 kN/mm^2 with respect to fibril axis (Table II) is given [12, 14]. This range is based on different experimental or theoretical methods used. Because the real cellulose modulus inside the fiber is not known, the presented results

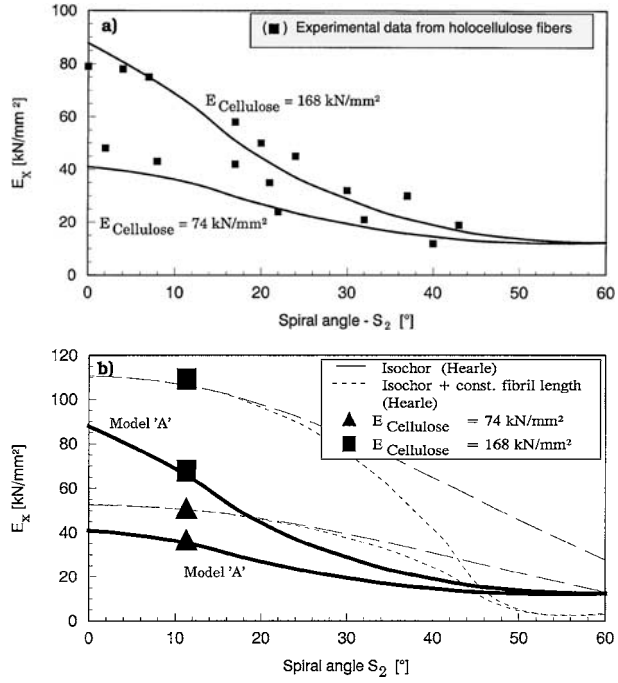

Figure 3 Correlation between the calculated and measured [6] elastic modulus (cellulose content = 65 wt.-%, spiral angle of S_1 and $S_3 = 70°$, relative thickness of the layers: P = 8%, S_1 = 8%, S_2 = 76%, S_3 = 8%). (a) Comparison with holocellulose fiber data [6]. (b) Comparison to Hearle's equations.

of our calculations are given for the above-mentioned possible range.

Fig. 3a illustrates together with some experimental data for holocellulose fibers [6] the calculated elastic modulus by using model A, assuming that the fibers were lignin-free with a cellulose content of 65 wt.-% typical for natural fibers (Table I). The relative thickness of the different layers were chosen to P = 8%, S_1 = 8%, S_2 = 76%, and S_3 = 8%. It can be seen in general, that the elastic modulus decreases with increasing spiral angle. The shape of the calculated curves is very similar to that published by Salmén *et al.* [6]. By comparing calculated and experimental data, a good correlation between both was obtained.

A further comparison with the well-known Hearle's equations [1–4] which only take into account the deformation mechanisms of the S_2 layer as the thickest one (with 76% of the whole fiber) with the calculated values by model 'A' is given in Fig. 3b. It can be seen for small spiral angles that the calculated values with model A are lower than in the case for Hearle's model because of the typically much higher real spiral angles for the S_1 and S_3 layers than for S_2. For different wood species spiral angles for $S_1 = 50°$ to 70°, $S_2 = 10°$, and $S_3 = 60°$ to 90° are published [5]. For natural fibers spiral angles for the S_2 layers (Table I) between 6–10° for jute, flax and hemp as the stiffest fibers, up to 10–22° for sisal, and 30–49° for coir are published [10, 11]. As already stated by Hearle, the curve shapes for spiral angles above 20° and 45° for isochoric deformations and isochoric + constant fibril length model, respectively, are not very close to the measured data, for instance according to Salmén *et al.* [6, 7].

As discussed previously, model A is based on laminated plate theory and is not able to consider the

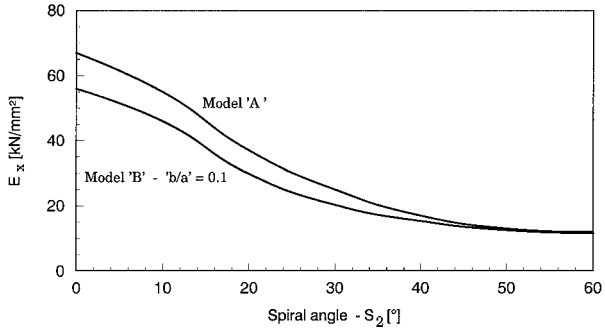

Figure 4 Comparison between model A and B (cellulose content = 53 wt.-%, spiral angle of S_1 and $S_3 = 70°$, relative thickness of the layers: P = 8%, $S_1 = 8\%$, $S_2 = 76\%$, $S_3 = 8\%$, $E_{cellulose} = 134$ kN/mm^2).

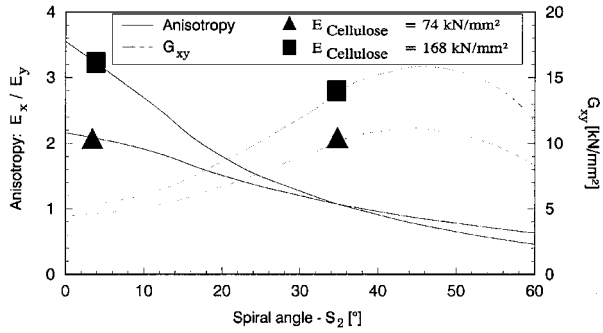

Figure 5 Influence of spiral angle on the degree of anisotropy and shear modulus of a natural fiber cell calculated by model A (cellulose content = 65 wt.-%, spiral angle of S_1 and $S_3 = 70°$, relative thickness of the layers: P = 8%, $S_1 = 8\%$, $S_2 = 76\%$, $S_3 = 8\%$).

elliptical cross section of the fiber, while model B does. If $b/a = 0.1$, the cross section and results of the calculations of model B strive to the results of model A with smaller differences which base on these geometrical aspects (Fig. 4).

The calculations of the degree of anisotropy of a natural fiber cell by using model A is shown in Fig. 5. It can be seen that the degree of anisotropy ranges from 2.2 up to 3.6 for a spiral angle of 0° dependent of cellulose modulus used, while an increasing angle leads to a general decrease in anisotropy. For spiral angles higher than approximately 30°, the difference in the degree of anisotropy is more or less independent on cellulose modulus used.

Furthermore, shear modulus, G_{xy}, versus spiral angle is also shown in Fig. 5. For spiral angles close to 0° a modulus of approximately 5 kN/mm^2 was calculated which is nearly independent of cellulose modulus used. Increasing spiral angle leads to an increase in shear modulus with an expected maximum at a spiral angle of 45°. By using 168 kN/mm^2 as cellulose modulus, the theoretical maximum shear modulus was calculated to 16 kN/mm^2, while using 74 kN/mm^2 as cellulose modulus resulted in a value of approximately 10 kN/mm^2.

3.2. Cellulose content dependency

Cellulose content is the second important structure property which affects significantly the overall mechanical properties of natural fibers. Typically, experimental

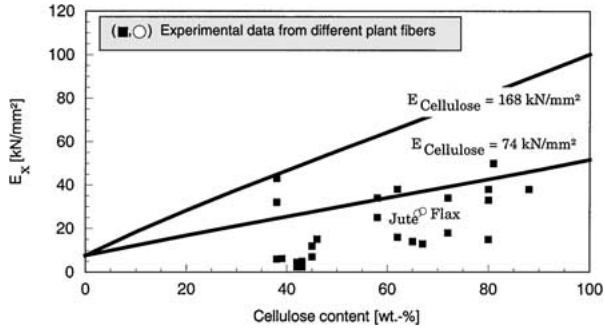

Figure 6 Correlation between the calculated and measured [10, 11] elastic modulus dependent on cellulose content. (Calculation: spiral angle of $S_1 = S_3 = 70°$ and $S_2 = 10°$, relative thickness of the layers: P = 8%, $S_1 = 8\%$, $S_2 = 76\%$, $S_3 = 8\%$, model A).

data [10, 11] were fitted by a trend line which from a theoretical point of view is based on a linear rule of mixture. A similar linear trend for fiber cell modulus with respect to fiber axis was calculated by using model A as shown in Fig. 6. These calculations were done with a spiral angle of the S_2 layers with 10° for jute, hemp or flax fibers. This spiral angle was chosen because it is well-known from x-ray analysis that this angle is approximately that of the stiffest natural fibers which are flax and hemp as well as jute.

Fig. 6 further illustrates a general comparison of fiber modulus E_x between calculated and experimental data of different types of natural fibers [16], neglecting other structural features like spiral angle. This neglect leads to the large spread of modulus for a given cellulose content. By using 74 kN/mm^2 for cellulose modulus, the curve is seen to fit the experimental data successfully.

In the previous chapter, the effects of the spiral angle on the fiber cell modulus was discussed in detail and it seems to be necessary to take these into consideration. The calculations in Fig. 6 were done for the structural parameters which are typical for jute and flax fibers. Comparing the experimental data of these two fibers with the calculated values shows that the theoretical calculated values are higher or much higher, dependent on cellulose modulus used, than the measured ones.

As shown in Fig. 6, real cellulose content of natural fibers stirs between approximately 40 up to 90 wt.-%. In this range, the calculated degree of anisotropy is, from the theoretical point of view, more or less independent of cellulose content for both cellulose modulus values used (Fig. 7). Shear modulus increases linear with increasing cellulose content with higher characteristic values for the higher cellulose modulus.

3.3. Dependency of cross section

The geometrical nature of natural fibers is typically based on an elliptic cross-section [2, 6, 7, 12, 14], schematically drawn in Fig. 2. Due to this fact, Fig. 8 illustrates the influence of the elliptical degree on the fiber cell's modulus in fiber axis. It can be seen that this characteristic value is greatly affected up to a geometry of $b/a = 0.4$ but is more or less constant afterwards. From practical point of view it is interesting to mention that the elastic modulus of the fiber cell is lower for circular cross section based fibers than for fibers with

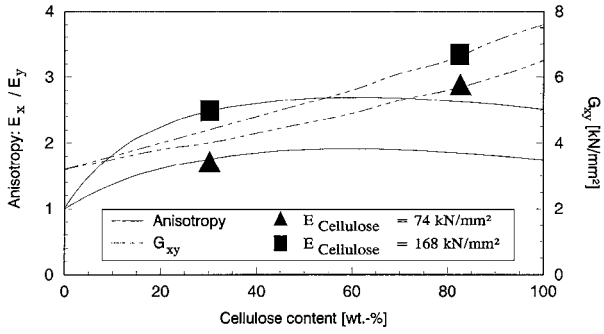

Figure 7 Influence of cellulose content on fiber cell anisotropy and shear modulus (spiral angle of $S_1 = S_3 = 70^\circ$ and $S_2 = 10^\circ$, relative thickness of the layers: $P = 8\%$, $S_1 = 8\%$, $S_2 = 76\%$, $S_3 = 8\%$, model A).

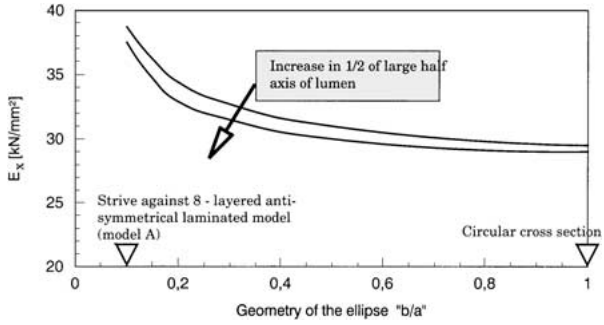

Figure 8 Influence of cell geometry and half axis size on the fiber cell moduls calculated by model B (cellulose content = 53 wt.-%, spiral angle of $S_1 = S_3 = 70^\circ$, $S_2 = 20^\circ$, relative thickness of the layers: $P = 8\%$, $S_1 = 8\%$, $S_2 = 76\%$, $S_3 = 8\%$, $E_{\text{cellulose}} = 134$ kN/mm^2).

a cross section with a high elliptic degree, i.e., small b/a-values.

From literature [2, 6, 7, 12,14] and the SEM study on jute fibers (Fig. 1) could be seen that a realistic b/a value should be higher than 0.6. Due to this fact, the studies by using model A about the effects of spiral angle and cellulose content on elastic properties in the previous sections are approximately 30% too high. This could be a further reason for the results in Fig. 6 and the poorer agreement between calculated and experimental data.

Nevertheless, tendencies between structural parameters and elastic properties are not influenced by this.

4. Conclusions

Two models were developed to calculate the elastic properties of natural fibers. Model A based on anti-symmertrical laminated structure, while model B based on a thick laminated composite tube model. Model B was able to take into account the elliptic geometry and hollow structure of the cross section of the fiber cell.

The calculated relationships between spiral angle and modulus in fiber axis by model A fitted successful experimental data for holocellulose fibers which were published elsewhere. The correlation with model A was much better as was found by using Hearle's equations, because Hearle's theory only took into account the paramaters of the S_2 layers.

In general, modulus in fiber axis decreases with increasing spiral angle as well as the degree of anisotropy, while shear modulus reached a maximum value for a spiral angle of 45°.

Fiber cell modulus increases linear with increasing cellulose content for both, the calculated (model A) and measured values. The correlation between experimental data and calculation was not a high as was shown in the case of modulus versus spiral angle. This may be explained by the fact, that the nature of a fiber cell is not as elliptic as supposed by the model A as SEM studies showed. The discrepancy between model A and a more real cross section was calculated (model B) with approximately 30%.

Furthermore, the degree of anisotropy is only slightly affected by the cellulose content in the range between 35 and 90%, which is the typical content for most natural fibers.

Acknowledgement

The authors wish to express their gratitude to BMBF-Bonn for financial support (Project-No. 96NR007-F and WTZ-LET010.97). Thanks also to the Latvian Ministry of Education and Science (Grant 6292/98) for its generous support of this paper.

References

1. J. HEARLE, *J. Appl. Polym. Sci.* **7** (1963) 1207.
2. *Idem.*, *ibid.* **7** (1963) 1635.
3. *Idem.*, *J. Polym. Sci.: Part C* **20** (1967) 215.
4. J. HEARLE and J. T. SPARROW, *J. Appl. Polym. Sci.* **24** (1979) 1857.
5. D. DINWOODIE, "Wood: Nature's Cellular, Polymeric Fibre-Composites" (The Institute of Metals, 1989).
6. L. SALMÉN and A. DE RUVO, *Wood and Fiber Science* **17**(3) (1985) 336.
7. L. SALMÉN, P. KOLSETH and M. RIGDAHL, in "Composite Systems from Natural and Synthetic Polymers," edited by L. Salmén, A. de Ruvo, J. C. Seferis and E. B. Stark (Elsevier Science Publishers B. V., Amsterdam, 1986) p. 211.
8. M. KOPONEN, T. TORATTI and P. KANERVA, *Wood Science & Technology* **23** (1989) 55.
9. *Idem.*, *Wood and Fiber Science* **25** (1991) 25.
10. E. C. MCLAUGHLIN and R. A. TAIT, *J. Mater. Sci.* **15** (1980) 89.
11. K. G. SATYANARAYANA, C. K. S. PILLAI, K. SUKUMARAN, S. G. K. PILLAI, R. K. ROHATGI and K. VIJAYAN, *ibid.* **17** (1982) 2453.
12. J. GASSAN, Dissertation at the Institute of Materials Engineering, University of Kassel, Kassel, 1997.
13. N.-S. HON, *J. Appl. Polym. Sci.* **37** (1983) 845.
14. H. P. FINK, J. GANSTER, J. FRAATZ and M. NYWLT, Akzo-Nobel Viskose Chemistry Seminar-Challenges in Cellulosic Man-Made Fibers, Stockholm, 30.5.–3.6.1994.
15. R. RIKARDS, A. CHATE and A. KORJAKIN, *Engineering Computation* **12** (1995) 61.
16. R. RIKARDS and A. CHATE, *Mechanics of Composite Materials and Structures* **4** (1997) 209.
17. H. ALTENBACH, J. ALTENBACH and R. RIKARDS, "Einführung in die Mechanik der Laminat- und Sandwichtragwerke" (Deutscher Verlag der Grundstoffindustrie, Stuttgart, 1996).
18. ZIENKIEWICZ, "The Finite Element Method" (MacGraw Hill, London, 1997).

Received 24 May 2000
and accepted 27 February 2001